Drug Development and Industrial Pharmacy, 2010; 36(10): 1177–1185

informa
healthcare

ORIGINAL ARTICLE

Insulin nanoparticles for transdermal delivery: preparation and physicochemical characterization and in vitro evaluation

Xiuhua Zhao, Yuangang Zu, ShuChong Zu, Dan Wang, Ying Zhang and Baishi Zu

Key Laboratory of Forest Plant Ecology, Northeast Forestry University, Ministry of Education, Harbin, Heilongjiang, China

Abstract

Aim: This work is aimed to study the feasibility of insulin nanoparticles for transdermal drug delivery (TDD) using supercritical antisolvent (SAS) micronization process. *Methods:* The influences of various experimental factors on the mean particle size (MPS) of insulin nanoparticles were investigated. Moreover, the insulin nanoparticles obtained were characterized by scanning electron microscopy (SEM), dynamic light scattering (DLS), Fourier-transform infrared spectroscopy (FTIR), X-ray diffraction (XRD), differential scanning calorimetry (DSC), and thermogravimetric (TG) analyses. *Results:* Under optimum conditions, uniform spherical insulin nanoparticles with a MPS of 68.2±10.8 nm were obtained. The Physicochemical characterization results showed that SAS process has not induced degradation of insulin. Evaluation in vitro showed that insulin nanoparticles were accorded with the Fick's first diffusion law and had a high permeation rate. *Conclusion:* These results suggest that insulin nanoparticles can have a great potential in TDD systems of diabetes chemotherapy.

Key words: *Insulin; nanoparticles; physicochemical characterization; preparation; transdermal delivery*

Introduction

It is understood that diabetes has become the third fatal disease after cardiovascular-cerebrovascular diseases and the cancer. Diabetes mellitus is caused by a decreased ability to use insulin or by decreased production of insulin, which results in decline of glucose levels[1]. Therefore, insulin is the most commonly used and the most important drug to treat diabetes mellitus patients in clinics[2].

Insulin is the only hormone protein that decreases glucose levels in the body. In the present study, the methods of drug delivery mostly include transdermal[3], nasal[4], pulmonary[5], buccal[6], ocular[7], and rectal[8]. However, there are some limitations to the delivery of insulin, such as short half-life, low permeation rates, and digestion by various proteolytic enzymes[9]. Transdermal delivery of insulin is an attractive method for the simple reason that it controls the release of drug and avoids possible enzymatic degradation resulting from gastrointestinal tract (GIT) of first-pass (gastric, intestinal, and hepatic) effects[10]. Nevertheless, the stratum corneum (skin's outermost layer) has a low permeability[11]. Therefore many attempts have been explored to enhance the permeation rates of insulin through skin, such as weakening the barrier with skin absorption enhancers[12], iontophoresis[13], ultrasound[14], and microneedles[15]. One such attempt is the micronization of drug particles.

Supercritical antisolvent (SAS) process is a new micronization technology developing in the recent years. It is suitable to prepare the micro- or nanoparticles because of low temperature and inertia[16]. The advantage of SAS process is that it is inexpensive, innocuous, and pollution-free. So far, more than 20 materials have successfully produced nanoparticles[17,18]. In this study, insulin nanoparticles were prepared by a SAS process. The insulin nanoparticles obtained were characterized by scanning electron microscopy (SEM),

Address for correspondence: Prof. Yuangang Zu, Key Laboratory of Forest Plant Ecology, Northeast Forestry University, Ministry of Education, Harbin, Heilongjiang 150040, China. Tel: +86 451 82191517. E-mail: zygorl@yahoo.com.cn

(Received 9 Sep 2009; accepted 11 Feb 2010)

ISSN 0363-9045 print/ISSN 1520-5762 online © Informa UK, Ltd.
DOI: 10.3109/03639041003695089

dynamic light scattering (DLS), Fourier-transform infrared spectroscopy (FTIR), X-ray diffraction (XRD), differential scanning calorimetry (DSC), thermogravimetric (TG) analyses and in vitro evaluation with the purpose of developing a suitable drug-delivery system of diabetes chemotherapy and transdermal drug delivery (TDD) systems of insulin.

Materials and methods

Materials

Dimethyl sulfoxide (DMSO, purity ≥ 99.5%) and insulin (purity ≥ 27 USP units/mg) made from bovine pancreas were supplied by Sigma-Aldrich (St. Louis, MO, USA). High purity CO_2 (purity ≥ 99.99%) was supplied by Liming Gas Company of Harbin (Harbin, PR China). These chemicals were used without further purification. Deionized pure water was prepared in our laboratory.

Methods

Apparatus and procedure

Figure 1 shows the schematic diagram of the SAS process apparatus. The CO_2 is cooled with a cooler (4) before being compressed by a liquid pump (8). The pressure is controlled by a backpressure-regulating valve. The CO_2 is then preheated in a heat exchanger (13), after which it enters the precipitation chamber (18). Simultaneously, the insulin DMSO solution is pumped, heated, and fed to the 1000 mL precipitation chamber through a stainless steel nozzle of 150 μm (16). A stainless steel frit vessel (17) of 200 nm is put into the precipitation chamber to collect the insulin nanoparticles and to let the SC–CO_2/DMSO mixture pass through. The flow rate of the mixture that leaves the precipitator is controlled by a valve (21) located between the precipitation chamber and the gas-liquid separation chamber (22). The liquid pump (6) is stopped when the fixed quantity of insulin DMSO solution is injected. Delivery of supercritical CO_2 is continued for 30 minutes to wash the frit vessel of the residual content of liquid solubilized in the supercritical antisolvent. Finally, the samples of insulin nanoparticles are taken from the frit vessel for further characterization analysis.

Optimization of SAS process

The orthogonal optimization experiment was carried out with four factors and four levels, namely A (concentration of insulin solution at 1.0, 1.5, 2.0, 2.5 mg/mL, respectively), B (drug solution flow rate at 3.3, 6.6, 9.9, 13.2 mL/min, respectively), C (precipitation pressure at 10, 15, 20, 25 MPa, respectively), and D (precipitation temperature at 40°C, 45°C, 50°C, 55°C, respectively). The range of each factor level was based on the results of preliminary experiments (Table 1). The mean particle size (MPS) (nm) of insulin nanoparticles was the dependent variable. The data was analyzed using the Design Expert 7.0 software. The significance level was stated at 95%, with *P*-value 0.05.

Powder characterization

Scanning electronic microscopy. SEM micrographs were taken using FEI Quanta 200 Environmental Scanning Electron Microscope (FEI Inc., Eindhoven, The Netherlands). Samples were coated by gold before examination (cathode dispersion).

Dynamic light scattering. The MPS of insulin nanoparticles was determined by a DLS equipment (ZetaPAL/90plus, Brookhaven Instruments, New York, NY, USA)

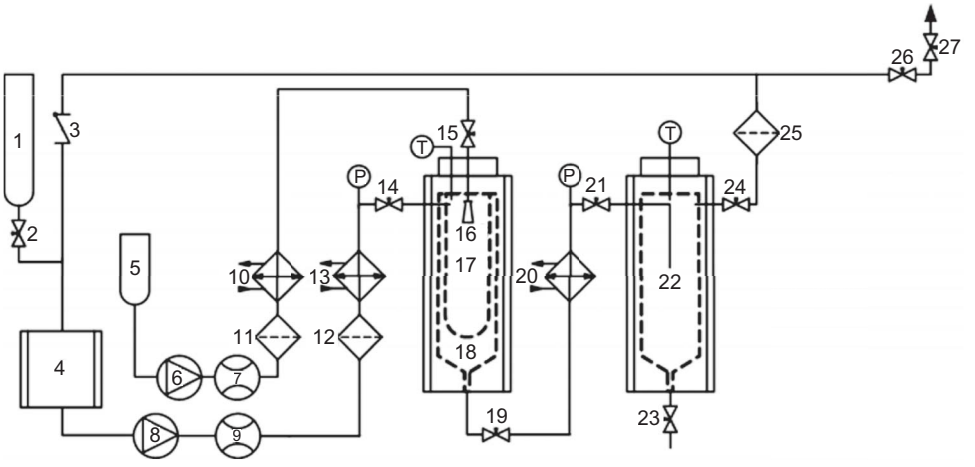

Figure 1. Schematic diagram of the apparatus. 1. CO_2 cylinder; 2, 14, 15, 19, 21, 23, 24, 26, and 27. Valves; 3. Check valve; 4. CO_2 cooler; 5. Liquid solution supply; 6. Liquid pump; 7 and 9. Flow meter; 8. CO_2 pump; 10, 13, and 20. Heat exchangers; 11, 12, and 25. Filters; 16. Nozzle; 17. Stainless steel frit vessel of 200 nm; 18. Precipitation chamber; 22. Gas-liquid separation chamber.

Table 1. The factors and levels of the orthogonal array design.

	A	B	C	D
Factor	Concentration of insulin solution (mg/mL)	Insulin solution flow (mL/min)	Precipitation pressure (MPa)	Precipitation temperature (°C)
Levels				
1	1.0	3.3	10	40
2	1.5	6.6	15	45
3	2.0	9.9	20	50
4	2.5	13.2	25	55

with a He-Ne laser (632.8 nm, 35 mW) as light source. Nanosuspension in filtered pure water was made for insulin particles. The water was pre-saturated with insulin to avoid dissolution of the nanoparticles. All the measurements were repeated three times. The MPS and standard deviations obtained were used to fit the particle size distribution to a lognormal distribution.

Fourier transform infrared spectrum. Chemical analyses of insulin samples were performed by FTIR spectroscopy using a MAGNA-IR560 E.S.P (Nicolet, Madison, WI, USA) instrument. The spectra were collected in transmission mode at room temperature in 4000–400 cm^{-1} range at a resolution of 2 cm^{-1}.

X-ray diffraction. Insulin particle crystallinity was analyzed using Xpert-Pro X-ray diffractometer (Philips; Xpert-Pro, Almelo, The Netherlands), with Cu Ka1 radiation generated at 30 mA and 50 kV. The XRD patterns were obtained in 2θ range of 3–80° using a 0.02° step size and 5°/min scan speed.

Differential scanning calorimetry and thermogravimetric analysis. The thermal property of proteins was analyzed with differential scanning calorimeter (DSC 204; TA instruments, New Castle, DE, USA). A sample of about 2 mg was sealed in an aluminum standard pan and then heated at a fixed temperature increment of 5°C/min and a temperature range of 30–200°C. The thermal stability of unprocessed and SAS-prepared samples was tested with a thermogravimetric analyzer (Diamond TG/DTA Perkin-Elmer, Waltham, MA, USA). During the course of testing, the samples weighing 2–3 mg were heated at a fixed heating rate of 10°C/min from 20°C to 500°C under a nitrogen purge.

Ex vivo permeation studies. The ex vivo percutaneous absorption experiments were performed on Wistar rat skin with Franz diffusion cells. A female Wistar rat (200–250 g) was sacrificed by excessive ether anesthesia and the hair was removed from the dorsal portion using an animal hair clipper. After harvesting the entire skin, the fat adhering on the dermis side was removed using a scalpel and 0.1% trypsin solution. Finally, the skin was washed in physiological saline and stored at –20°C in aluminum foil packing. The intactness of the skin was tested with a 0.1% methylene blue solution on the donator site using a stereoscope. Rat skin was mounted on cells with a surface area of 1.766 cm^2 and a receiver compartment filled with 12 mL phosphate-buffered saline (0.1 M; pH 7.4). The receiver fluid was continuously stirred with a stirring speed of 1000 rpm and maintained at 37 ± 1°C. The water-dispersing solution with concentration of 0.4 and 5 mg/mL (containing 5% glycerol) of raw and insulin nanoparticles were applied to the epidermal surface. The receiver fluid was removed 3 mL at a time at 0.5, 1, 1.5, 2, 3, 4, 5, and 6 hours and supplied with the same volume of fresh receiver solution. The concentrations of insulin in receiver fluid samples were determined using a waters HPLC system consisting of a pump (Model 1525), an auto-sampler (Model 717 plus), UV detector (Waters 2487 Dual λ Absorbance Detector) at 214 nm. The C18 column (Diamonsil, 5 μm, 4.6 mm × 250 mm, Dikma Technologies) was used at 25 ºC. The mobile phase consisted of 0.1 mol/L sodium phosphate-0.05 mol/L sodium sulphate-acetonitrile (35:35:30, v/v/v) delivered at 1.0 mL/min. The injection volume was 20 μL.

Results and discussion

Optimization study and morphology of insulin nanoparticles

The results of the experiment and the collected data for MPS of micronized insulin is shown in Table 2. The results in Table 2 indicate that the maximum MPS of insulin nanoparticles was 317.4 ± 20.9 nm, and the minimum was 81.5 ± 4.7 nm and the influence on the MPS of insulin nanoparticles decreases in the order: A>C>B>D according to the *R*-values. So the minimum MPS of insulin nanoparticles was obtained when concentration of insulin solution, drug solution flow rate, precipitation pressure, and precipitation temperature were $A_1B_3C_4D_1$ (1.0 mg/mL, 9.9 mL/min, 25 MPa, and 40°C), respectively. Through a confirmatory test, smaller micronized insulin was obtained, with a MPS of 68.2 ± 10.8 nm. Figure 2 shows that raw insulin particles are irregular lump crystals with length varying from 0.5 to 14.4 μm. It can be seen from Figure 3 that insulin nanoparticles are spherical.

Table 2. Orthogonal array design $OA_{16}(4)^5$ and experimental results.

Trial no.	A	B	C	D	CO_2 flow rate (kg/h)	MPS(nm) ± SD (n=3)
1	1	1	1	1	12.0	106.0 ± 6.6
2	1	2	2	2	12.0	130.3 ± 9.0
3	1	3	3	3	12.0	81.5 ± 4.7
4	1	4	4	4	12.0	141.5 ± 5.3
5	2	1	2	3	12.0	228.9 ± 7.6
6	2	2	1	4	12.0	275.2 ± 21.3
7	2	3	4	1	12.0	132.8 ± 6.3
8	2	4	3	2	12.0	240.9 ± 9.0
9	3	1	3	4	12.0	195.4 ± 10.1
10	3	2	4	3	12.0	169.0 ± 8.3
11	3	3	1	2	12.0	262.8 ± 13.4
12	3	4	2	1	12.0	281.5 ± 8.8
13	4	1	4	2	12.0	247.8 ± 17.4
14	4	2	3	1	12.0	218.5 ± 15.7
15	4	3	2	4	12.0	291.1 ± 20.3
16	4	4	1	3	12.0	317.4 ± 20.9
K_1[a]	114.8 ± 6.4	194.5 ± 10.4	240.4 ± 15.6	184.7 ± 9.4		
K_2	219.5 ± 11.1	198.3 ± 13.6	233.0 ± 11.4	220.5 ± 12.2		
K_3	227.2 ± 10.2	192.1 ± 11.2	184.1 ± 9.9	199.2 ± 10.4		
K_4	268.7 ± 18.6	245.3 ± 11.0	172.8 ± 9.3	225.8 ± 14.3		
R[b]	153.9	53.3	67.6	41.1		
Optimal level	A_1	B_3	C_4	D_1		

[a]K_i^A = Σ(mean particle size at Ai)/4, the mean values of mean particle size for a certain factor at each level with standard deviation. [b]R_i^A = max K_i^A − min K_i^A.

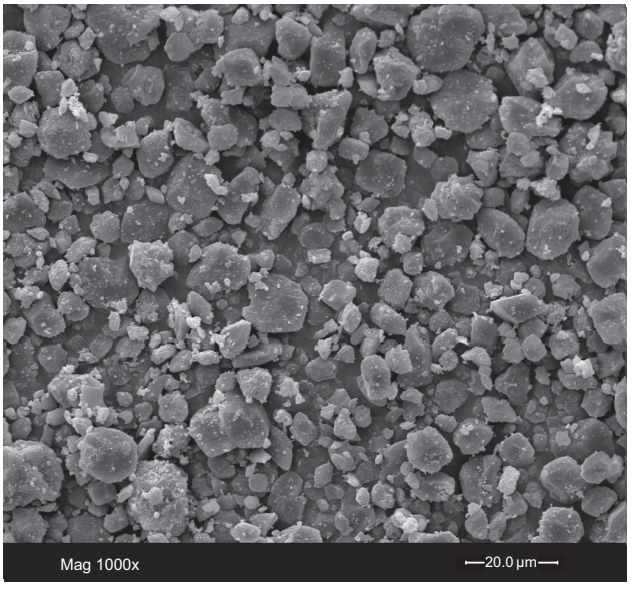

Figure 2. SEM image of raw insulin.

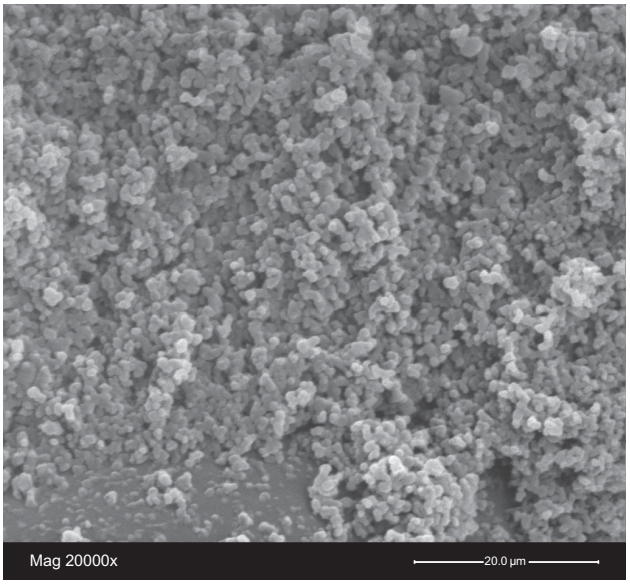

Figure 3. SEM images of nano insulin precipitated from DMSO under optimum condition.

Effect of the process parameters

In this study, ultra-fine insulin particles were prepared with the SAS apparatus by using DMSO as a solvent and carbon dioxide as an antisolvent. The relationships between the MPS of ultra-fine insulin particles and different process parameters are shown in Figure 4. Table 3 lists the data of the analysis of variance (ANOVA) table of this experiment. The influences of several process parameters on the MPS of the particulate products are discussed as followed.

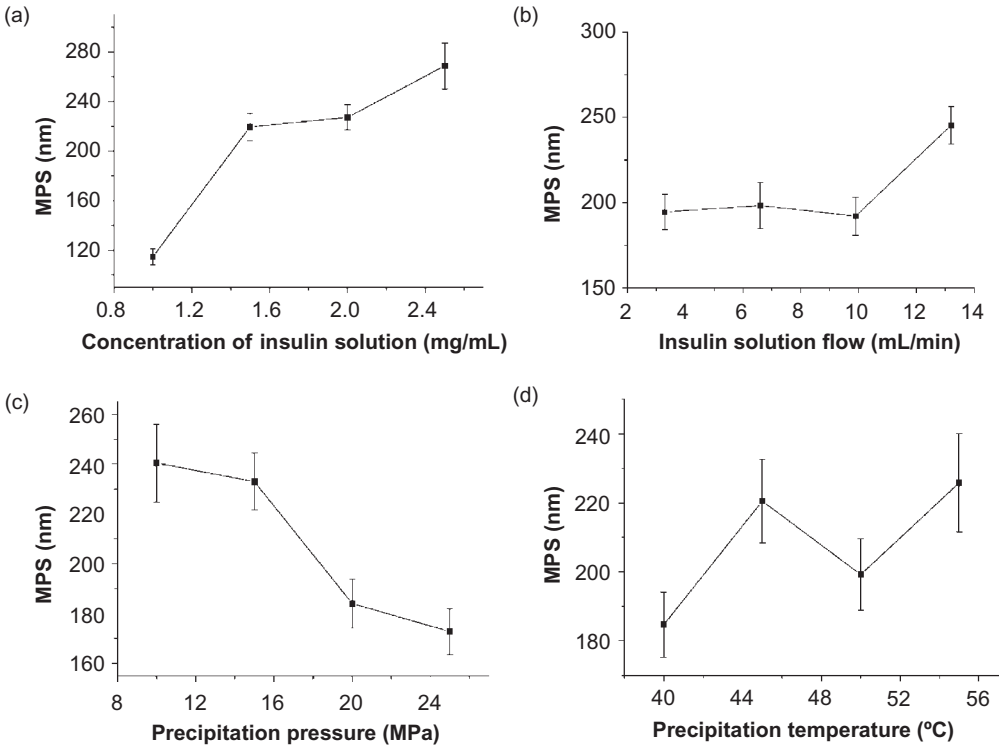

Figure 4. The effect of each parameter on the MPS of micronized insulin. Error bar shows standard deviations for $n = 3$. (a) Concentration of insulin solution; (b) Insulin solution flow rate; (c) Precipitation pressure; (d) Precipitation temperature.

Table 3. ANOVA analysis of four parameters for SAS process of insulin.

Source	Sum of squares (SS)	Degrees of freedom (df)	*F*-ratio	$F_{0.05}$	Type of effect
(A) Concentration of insulin solution	51,455.992	3	29.143	9.280	Significant
(B) Insulin solution flow rate	7693.362	3	4.357	9.280	
(C) Precipitation pressure	13,925.502	3	7.887	9.280	
(D) Precipitation temperature	4365.267	3	2.472	9.280	

Figure 4a shows the effect of the concentration of insulin solution (1.0, 1.5, 2.0, and 2.5 mg/mL) on the MPS of particulate products. As shown in the figure, the MPS increased with increasing concentration. According to the atomization and droplet broken mechanism, the increase of insulin solution concentration results in the increase of the viscosity and surface tension of the mixture in the precipitation chamber, which increases the thickness of the liquid film and the drag coefficient between the droplet and the gas phase. These factors would lead to an imperfect atomization and the droplet tends to turn into disc-shaped objects. Based on the concept of 'one droplet one particle'[19], the large particles are formed at high concentration of insulin solution. The concentration of insulin solution was appraised as a significant factor, based on ANOVA with 95% confidence.

Figure 4b shows the effect of drug solution flow rate (3.3, 6.6, 9.9, and 13.2 mL/min) on the MPS of particulate products. As shown in the figure, the MPS remained constant when the drug solution flow rate increased from 3.3 to 9.9 mL/min, and increased significantly from 9.9 to 13.2 mL/min. With the increase of the drug solution flow rate the mass flow rate of the liquid mixture increases, which leads to the increase in the thickness of the liquid film. Therefore, the droplet formed by the SAS process becomes large and the particles precipitated in the precipitator become large based on the mechanism of 'one droplet one particle'.

Figure 4c shows the effect of precipitation pressure (10, 15, 20, and 25 MPa) on the MPS of particulate products. As shown in the figure, the MPS decreased with increasing pressure. The explanation for this effect is related to the enhancement in solvent power of SC–CO_2 with increasing pressure that will reduce the solvation sphere of the DMSO molecules and, consequently, decrease the possibility of interaction between DMSO and insulin. At the same time, with the increase of the pressure in the precipitation chamber, the content of CO_2 in the liquid solution increases rapidly, while the viscosity and the surface tension of the mixture in the precipitation chamber reduce. The atomization becomes more violent

and the primary droplets formed become smaller, which results in the precipitation of smaller particles. Therefore, when the pressure increases, the MPS becomes smaller. However precipitation pressure was not identified as a significant factor for insulin micronization, based on ANOVA.

Figure 4d shows the effect of precipitation temperature (40°C, 45°C, 50°C, and 55°C) on the MPS of particulate products. In this study, the precipitation temperature does not significantly affect the MPS. The influence of the precipitation temperature on the process is in two ways: one is that the viscosity of the mixture in the precipitation chamber decreases with the increase of the temperature, the other is that the increase of the temperature results in decreasing of CO_2 content in the liquid solution. These two opposite effects might offset each other and weaken the effect of temperature on the atomization of the liquid mixture in the precipitation chamber and the formation of the particles to a certain extent. Therefore, the influence of the precipitation temperature on the MPS is not remarkable.

Physicochemical characterization

The molecular structures of raw and nano insulin were examined with FTIR. FTIR spectra (see supplementary Figure S1 available online at http://informahealthcare.com/doi/suppl/[doinumber]) show the presence of the following speaks: 3320, 2959, 1657, 1517, 1241, and 617 cm^{-1}. No significant differences were observed between the two samples.

XRD analyses of raw and nano insulin were performed to evaluate the occurrence of eventual structural changes at the crystal level. Figure 5 shows that raw insulin has two weak broad peaks (at 2θ = 9.5° and 22.3°), revealing that the raw insulin samples have low crystallinity. However, the XRD spectrum of nano insulin shows only one broad peak (at 2θ = 22.3°) compared to raw insulin. The disappearance of diffraction peak at 9.5° is attributed to the reduced particle crystallinity or the decrease in the particle size.

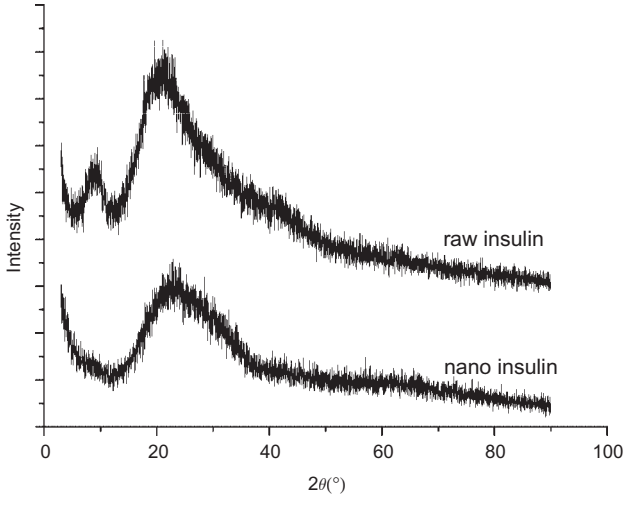

Figure 5. XRD patterns of raw and nano insulin (nano insulin is the micronized insulin precipitated from DMSO under optimum condition).

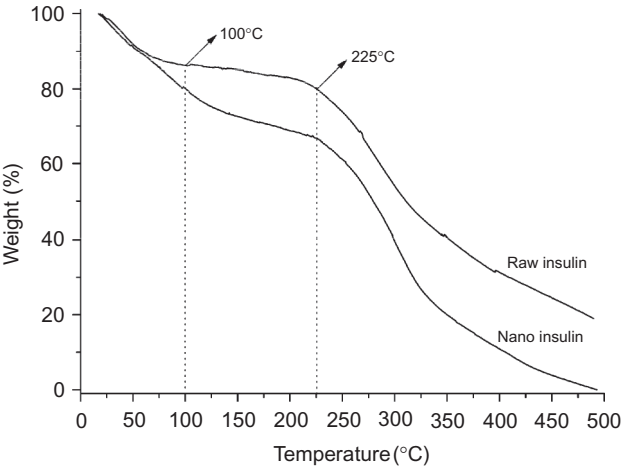

Figure 6. TGA results of insulin powders. (a) Raw insulin; (b) Nano insulin (nano insulin is the micronized insulin precipitated from DMSO under optimum condition).

The TGA results, used to examine the thermal property of nano insulin, are shown in Figure 6. Raw insulin is observed to moderately lose weight from 20°C to 100°C, due to its water loss. Then its weight decreases quickly from about 225°C, due to its strong vaporization, followed by its decomposition. However, the TGA result of nano insulin shows higher weight loss percentage compared to raw insulin at the same temperature. It is possibly due to the fact that nano insulin with small MPS has higher specific surface area and hence has higher specific surface energy, which subsequently leads to an easier vaporization and earlier decomposition energy. Similar results have been reported in other papers[20].

To further confirm the physical state of insulin samples, DSC test was preformed (Figure 7). The thermogram of raw and nano insulin show one broad endothermic peak around 72.93°C (the enthalpy change of this peak was ΔH = 98.9174 J/g) and 63.11°C (ΔH = 50.9765 J/g), respectively, which is due to water loss. It agrees with TG analysis. The difference observed for thermogram may be due to lower crystallinity or higher specific surface energy of nano insulin, which subsequently leads to an easier water loss.

Percutaneous absorption of insulin nanoparticles

The ex vivo percutaneous absorption experiments were performed on Wistar rat skin with Franz diffusion cells.

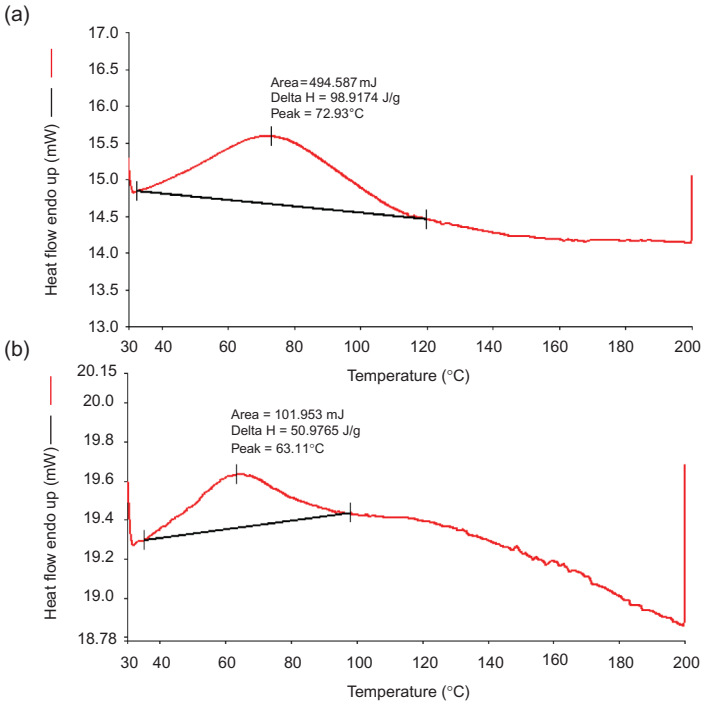

Figure 7. DSC patterns of raw and nano insulin. (a) Raw insulin; (b) Nano insulin (nano insulin is the micronized insulin precipitated from DMSO under optimum condition).

The intactness of the skin was tested with 0.1% methylene blue solution on the donator site using a stereoscope before the percutaneous experiment. Figure 8a–c are the photographs of the original rat skin (undyed), intact skin, and damaged skin. Two experimental groups (concentration of 0.4 and 5 mg/mL) were carried out with intact skin. The penetration of insulin dispersion into phosphate-buffered saline (0.1 M; pH 7.4) through rat skin was investigated over 6 hours. Each sample was analyzed in triplicate. Figure 9 shows the penetration profile of raw and nano insulin suspension. According to Figure 9, the process of percutaneous absorption is a uniform acceleration release. There is a linear relationship between accumulation penetration count and time, the permeation coefficient of raw and nano insulin are 0.52 and 14.47 μg/cm^2/h (5 mg/mL), 1.26 and 10.79 μg/cm^2/h (0.4 mg/mL), respectively. Insulin nanoparticles were accorded with the Fick's first diffusion law and had a high permeation rate. Figure 10 shows the particle size distribution of insulin penetrating fluids accordingly. As can be seen from the figure, the MPS of raw and nano insulin water-dispersing solution containing 5% glycerol are 4612.0 and 201.8 nm, respectively. This fact indicates that the increase of permeance and penetration rate may be due to the decrease of the MPS of nano insulin. These results suggest that insulin nanoparticles can have a great potential in TDD systems of diabetes chemotherapy.

Conclusion

In conclusion, uniform spherical insulin nanoparticles with a MPS of 68.2 ± 10.8 nm were obtained by SAS process. Moreover, insulin nanoparticles were characterized by SEM, DLS, FTIR, XRD, DSC, and TG analyses. The

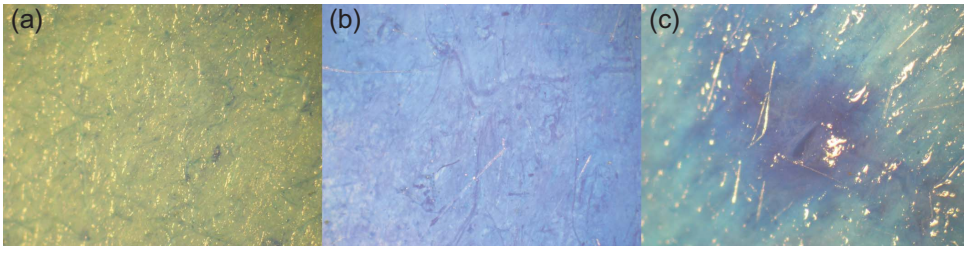

Figure 8. Photographs of the Wistar rat skin. (a) Original rat skin (undyed); (b) Intact skin (tested with 0.1% methylene blue solution); (c) Damaged skin (tested with 0.1% methylene blue solution).

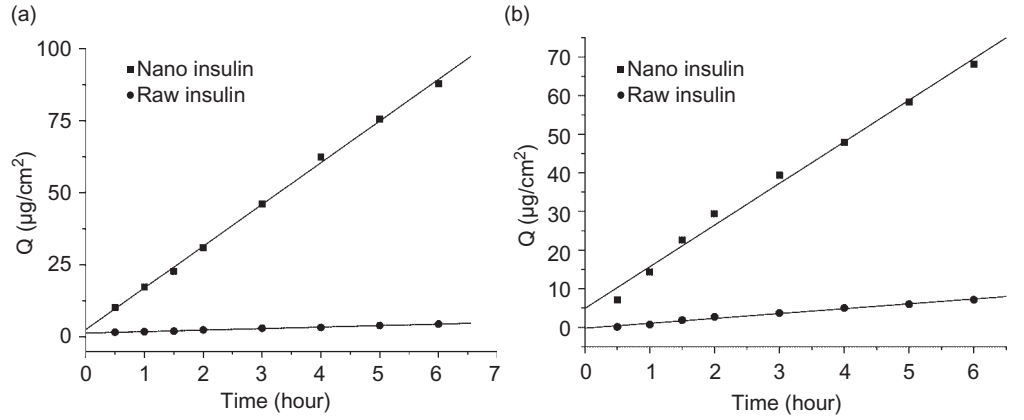

Figure 9. Percutaneous absorption of raw and nano insulin (nano insulin is the micronized insulin precipitated from DMSO under optimum condition). (a) 5 mg/mL; (b) 0.4 Smg/mL.

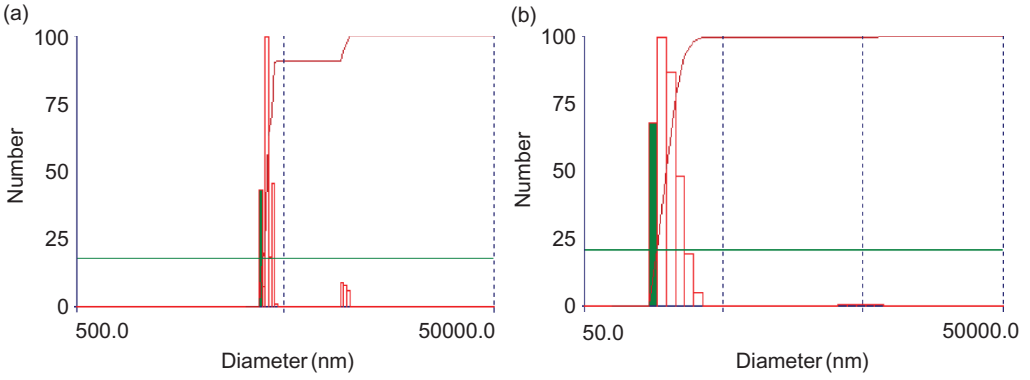

Figure 10. Particle size distribution of penetrating fluids. (a) Raw insulin (water dispersing solution containing 5% glycerol); (b) nano insulin (water dispersing solution containing 5% glycerol).

results showed that SAS process has not induced degradation of insulin. Evaluation in vitro showed that insulin nanoparticles were accorded with the Fick's first diffusion law and had a high permeation rate. These results suggest that insulin nanoparticles can have a great potential in TDD systems of diabetes chemotherapy.

Acknowledgments

The authors gratefully acknowledge the support of the National Key Technology R&D Program (2006BAD 18B0401), the Fundamental Research Funds for the Central Universities (DL09BB08) and Program of Science and Technology from State Forestry Administration (2007–12). Mr. Yongzhi Cui would be greatly appreciated for SEM analysis.

Declaration of interest

The authors report no conflicts of interest. The authors alone are responsible for the content and writing of this paper.

References

1. Gale EAM. (2009). The discovery of type 1 diabetes. Diabetes, 50(2):217–26.
2. Vivian Fonseca M. (2006). The role of basal insulin therapy in patients with type 2 diabetes mellitus. Insulin, 1(2):51–60.
3. Chen H, Zhu H, Zheng J, Mou D, Wan J, Zhang J, et al. (2009). Iontophoresis-driven penetration of nanovesicles through microneedle-induced skin microchannels for enhancing transdermal delivery of insulin. J Control Release, 139(1):63–72.
4. Skyler JS, Weinstock RS, Raskin P, Yale JF, Barrett E, Gerich JE, et al. (2005). Use of inhaled insulin in a basal/bolus insulin regimen in type 1 diabetic subjects: A 6-month, randomized, comparative trial. Diab Care, 28(7):1630–5.
5. Klingler C, Müller BW, Steckel H. (2009). Insulin-micro- and nanoparticles for pulmonary delivery. Int J Pharm, 377(1–2): 173–9.
6. Singh B, Chauhan N. (2009). Modification of psyllium polysaccharides for use in oral insulin delivery. Food Hydrocolloid, 23(3):928–35.
7. Lee Y-C, Simamora P, Pinsuwanc S, Yalkowskya SH. (2002). Review on the systemic delivery of insulin via the ocular route. Int J Pharm, 233(1–2):1–18.
8. Hosny EA (1999). Relative hypoglycemia of rectal insulin suppositories containing deoxycholic acid, sodium taurocholate, polycarbophil, and their combinations in diabetic rabbits. Drug Dev Ind Pharm, 25(6):745–52.
9. El-Sayed Khafagy MM, Onukia Y, Takayamaa K. (2007). Current challenges in non-invasive insulin delivery systems: A comparative review. Adv Drug Deliv Rev, 59(15):1521–46.

10. Prausnitz MR, Mitragotri S, Langer R. (2004). Current status and future potential of transdermal drug delivery. Nat Rev Drug Discov, 3(2):115–24.
11. Prausnitz MR, Mitragotri S, Langer R. (2001). Overcoming skin's barrier: The search for effective and user-friendly drug delivery. Diab Technol Ther, 3(2):233–6.
12. El Maghraby GM, Williams AC, Barry BW. (2004). Interactions of surfactants (edge activators) and skin penetration enhancers with liposomes. Int J Pharm, 276(1–2):143–61.
13. Kalia YN, Naik A, Garrison J, Guy RH. (2004). Iontophoretic drug delivery. Drug Deliv, 56(5):619–58.
14. Lavon I, Kost J. (2004). Ultrasound and transdermal drug delivery. Drug Discov Today, 9(15):670–6.
15. Prausnitz MR. (2004). Microneedles for transdermal drug delivery. Adv Drug Deliv, 56(5):581–7.
16. Reverchon E, Adami R. (2006). Nanomaterials and supercritical fluids. J Supercrit Fluids, 37(1):1–22.
17. Miguel AMF, Gamse T, Cocero MJ. (2006). Supercritical antisolvent precipitation of lycopene: Effect of the operating parameters. J Supercrit Fluids, 36(3):225–35.
18. Catchpole OJ, Grey JB, Mitchell KA, Lan JS. (2004). Supercitical antisolvent fractionation of propolis tincture. J Supercrit Fluids, 29(1–2):97–106.
19. Zhiyi L, Jingzhi J, Xuewu L, Huihua T, Wei W. (2009). Experimental investigation on the micronization of aqueous cefadroxil by supercritical fluid technology. J Supercrit Fluids, 48(3):247–52.
20. Huang Z, Sun G-B, Chiew YC, Kawi S. (2006). Formation of ultrafine aspirin particles through rapid expansion of supercritical solutions (RESS). Powder Technol, 160(2): 127–34.